

# Noncovalent Tailoring of the Binding Pocket of Self-Assembled Cages by Remote Bulky Ancillary Groups

Yu Fang, Takashi Murase, Sota Sato, and Makoto Fujita\*

Department of Applied Chemistry, School of Engineering, The University of Tokyo, 7-3-1 Hongo, Bunkyo-ku, Tokyo 113-8656, Japan

**S** Supporting Information

**ABSTRACT:** The binding properties of a self-assembled coordination cage were subtly tuned by ancillary groups on the metal corners of the cage. Since the bulky mesityl groups of the ligand hang over the cage cavity, the effective cavity volume is reduced. Due to the tighter guest packing inside the shrunken cavity, smaller guests were efficiently bound and guest motion was restricted even at high temperatures.

The elaborate substrate specificity in the binding pocket of enzymes is often governed by the subtle variation in amino acid residues that exist, not at the interior, but at the exterior of the pocket.<sup>1</sup> Two similar serine proteases, trypsin and chymotrypsin, have, for example, almost identical binding pockets but exhibit distinctly different substrate specificity<sup>2</sup> because of the difference in their surface loops that do not touch the substrates.<sup>3</sup> The role-separation of recognition and its regulation is nature's clever approach for specific guest binding, where the specificity can be finely tuned without changing the binding pocket structure itself. We report here that the binding properties of synthetic coordination cages **1** (Figure 1) can be

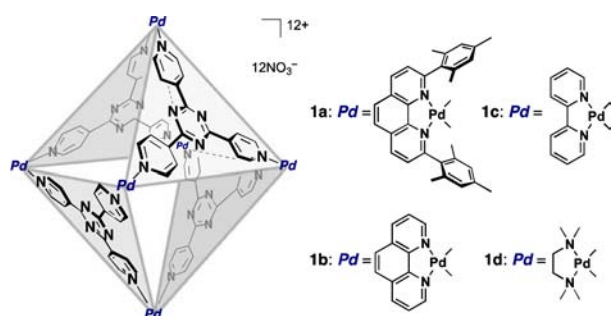


**Figure 1.** Self-assembled coordination cages **1**.

easily tailored by modifying the remote ancillary group on the component metal ions.<sup>4</sup> Since a variety of cis-chelating ligands can be employed as ancillary groups,<sup>5</sup> our approach provides the most efficient and straightforward way to subtly control the binding properties of the cages.

A bulky ancillary ligand, 2,9-dimesityl-1,10-phenanthroline (Mes-phen),<sup>6</sup> is employed to noncovalently control the binding of encapsulated guests. The bulky *cis*-protected Pd(II) complex, Pd(Mes-phen)(NO<sub>3</sub>)<sub>2</sub> (**2**), was prepared in high yield by treating PdCl<sub>2</sub> with Mes-phen followed by counterion exchange

with AgNO<sub>3</sub> and identified by NMR, MS, and X-ray analyses (see Figures S1–S5 in the Supporting Information). Complexation of **2** (20 mg, 31 μmol) with 2,4,6-tri(4-pyridyl)-1,3,5-triazine (**3**; 6.3 mg, 20 μmol) in H<sub>2</sub>O/CH<sub>3</sub>CN (4:1, 4.0 mL) at 60 °C for 1 h gave cage **1a** as a single product as confirmed by <sup>1</sup>H NMR spectroscopy (Figures 2b–d) and ESI-MS (Figure

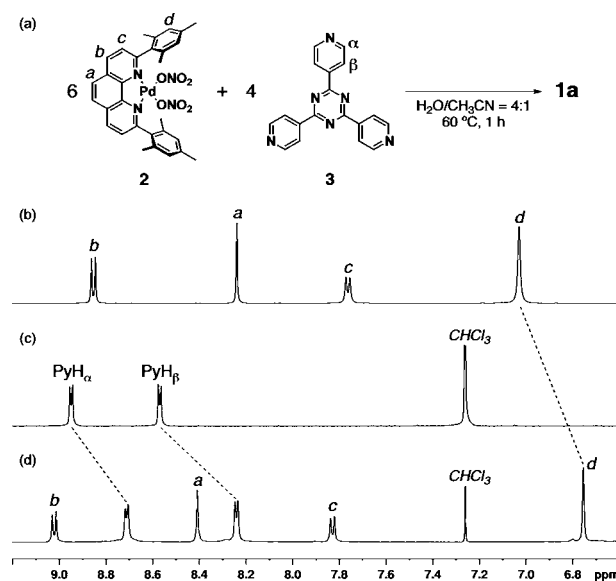


**Figure 2.** (a) Self-assembly of cage **1a** from bulky Pd(II) complex **2** and triazine panel ligand **3**. (b–d) <sup>1</sup>H NMR spectra (500 MHz, 300 K) of (b) Pd(II) complex **2** (in CD<sub>3</sub>CN), (c) triazine ligand **3** (in CDCl<sub>3</sub>), and (d) cage **1a** (in D<sub>2</sub>O). TMS (CDCl<sub>3</sub> solution) in a capillary served as an external standard ( $\delta = 0$  ppm) in D<sub>2</sub>O.

S24). Notably, the pyridyl protons (PyH $\alpha$  and PyH $\beta$ ) of triazine panel **3** shifted upfield (Figures 2c,d) in contrast to the common downfield shifts characteristic to pyridyl coordination to Pd(II) in the formation of cages **1b–d** (Figure S17). The unusual upfield shift is explained by the shielding effect of the mesityl groups of the Mes-phen ligand that hang over the pyridyl groups of the cage. The signals of the mesityl aromatic protons (H<sub>d</sub>) were also shifted upfield ( $\Delta\delta = -0.28$  ppm) due to the shielding by the pyridyl group (Figures 2b,d). These observations indicate a significant through-space interaction between the mesityl and the pyridyl groups in cage **1a**. After

**Received:** November 20, 2012

**Published:** December 27, 2012

anion exchange from  $\text{NO}_3^-$  to  $\text{PF}_6^-$ , ESI-MS clearly confirmed the  $\text{M}_6\text{L}_4$  composition of the cage with a molecular weight of 6126.75 Da.

The structure of cage **1a** ( $\text{PF}_6^-$  salt) was unambiguously determined by a synchrotron X-ray diffraction study (Figure 3).

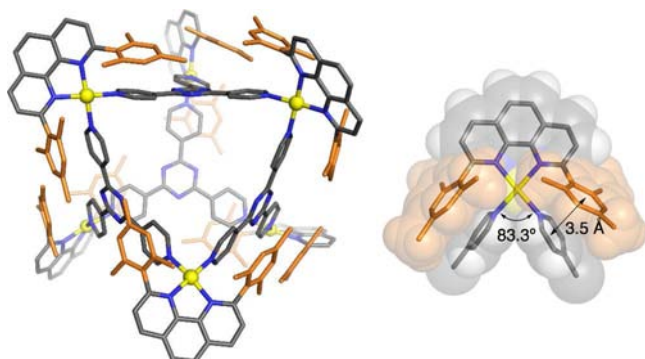


**Figure 3.** X-ray crystal structure of cage **1a** ( $\text{PF}_6^-$  salt). For clarity, H-atoms,  $\text{PF}_6^-$  counteranions, and solvent molecules have been omitted. C, gray; N, blue; Pd, yellow; mesityl group, orange. The coordination environment of the Pd(II) center is highlighted on the right with space-filling depiction in the background.

A block-shaped single crystal of **1a** ( $\text{PF}_6^-$  salt) was obtained by slow diffusion of ethanol into the acetonitrile solution at 15 °C for 2 d. The crystal structure shows that the two mesityl substituents in the Mes-phen ligand hang over the two remaining coordination sites on the Pd(II) center, narrowing the coordination bite angle.<sup>7</sup> At the same time, the mesityl groups interact through space with the pyridyl groups of the triazine-cored ligand **3** of the cage at a distance of  $\sim 3.5$  Å. Due to the steric demand of the mesityl groups, the pyridine rings of **3** are tilted by 9.4° on average with respect to the triazine core. Most importantly, the Pd(II) ions display a distorted square planar geometry and the average N–Pd–N bite angle defined by the two 4-pyridyl nitrogen atoms on every Pd(II) ion is 83.3° and significantly deviates from the ideal 90° angle.

We calculated the cavity volumes of cages **1a**, **1c**, and **1d** using the VOIDOO program<sup>8</sup> based on their crystal structures.<sup>9,10</sup> The cavity volumes occupied by a large sphere probe with a radius of 3.36 Å were measured and are visualized in Figure 4. While cages **1c** and **1d** have similar void volumes

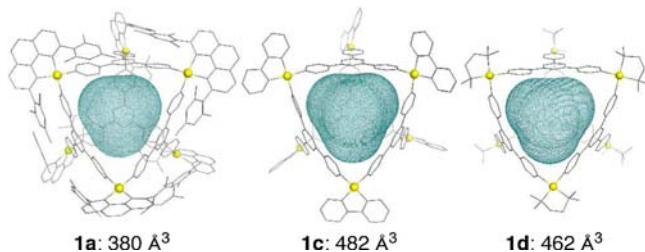


**Figure 4.** The central void volumes (green mesh) in cages **1a**, **1c**, and **1d**. Probe radius = 3.36 Å.

(482 and 462 Å<sup>3</sup>, respectively), cage **1a** shows a much smaller volume (380 Å<sup>3</sup>).<sup>11</sup> Thus, the cavity of cage **1a** is considerably reduced by the smaller N–Pd–N bite angles and the deformed ligand **3** with tilted pyridine moieties.

The guest-binding properties of cage **1a** were compared with those of cages **1b–d**, which form 1:4 host–guest complexes

with adamantane in water.<sup>12</sup> To our surprise, cage **1a** could no longer encapsulate adamantane in its cavity because of the shrunken cavity. In contrast, tetraphenylmethane (**4a**) is too small to be efficiently encapsulated in the large cavities of **1b–d** but was efficiently bound by **1a** to give the inclusion complex **1a·4a** in 56% yield.

A series of rigid tetrahedral guests **4a–d** (362–394 Å<sup>3</sup>) were also examined as probe molecules (Table 1). The inclusion

**Table 1.** Guest-Binding Specificity of Cages **1** for Tetrahedral Guests **4**<sup>a</sup>

Inclusion complex <b>1·4</b>	Guest <b>4</b>	size (Å <sup>3</sup> ) <sup>b</sup>	Inclusion yield (%) <sup>c</sup>			
			<b>1a</b>	<b>1b</b>	<b>1c</b>	<b>1d</b>
	M = C ( <b>4a</b> )	361.50	56	0	0	11
	M = Si ( <b>4b</b> )	374.46	75	0	0	12
	M = Ge ( <b>4c</b> )	382.73	43	0	0	12
	M = Sn ( <b>4d</b> )	393.75	38	0	0	19

<sup>a</sup>Conditions: cage **1** and guest (10 equiv) in D<sub>2</sub>O (1.0 mM) at 80 °C for 4 h unless otherwise noted. Excess guest was removed by filtration before NMR measurements. <sup>b</sup>van der Waals volumes calculated from structures optimized using SPARTAN<sup>10</sup> with MP2 using both a 6-31G\* and a larger 6-311+G\*\* basis set. <sup>c</sup>NMR yields.

yields are quite sensitive to subtle changes in both the host and guest structures. The highest inclusion yield was obtained for **1a·4b**, but the yields fall significantly with increasing cavity volume (**1a**  $\ll$  **1d**  $<$  **1b**  $\approx$  **1c**). The 2D NOESY NMR spectrum of inclusion complex **1a·4b** (Figure S34) indicated that **4b** is located at the cavity center with the four phenyl groups at the cavity portals. Interestingly, with guests **4c** and **4d**, which are slightly larger than **4b**, the inclusion yields decreased (43% and 38%, respectively).

Guest mobility largely depends on the cavity volumes of hosts **1**. Two molecules of diketone **5** are quantitatively encapsulated by cages **1a** and **1b** to form an orthogonally associated, S<sub>4</sub> symmetric dimer (**5**)<sub>2</sub> in the cavity.<sup>13</sup> In both cases, 12 sharp signals are observed in the <sup>1</sup>H NMR spectrum for triazine ligand **3** at 300 K because of the symmetry reduction of the host from T<sub>d</sub> to S<sub>4</sub> (Figures 5a,c).<sup>13</sup> With increasing temperature, the host signals of **1b·(5)**<sub>2</sub> gradually broaden, indicating the dissociation of the (**5**)<sub>2</sub> dimer (Figure 5d). In contrast, those of **1a·(5)**<sub>2</sub> remain sharp even at elevated temperatures (Figure 5b). This observation indicates that dimer (**5**)<sub>2</sub> fits more snugly and is confined in the shrunken cavity of cage **1a** even at high temperature.

In summary, we prepared self-assembled cage **1a** with Mes-phen ancillary ligands on the Pd(II) centers, where the cavity-forming ligand and the ancillary ligand cooperatively but independently play important roles: the former forms an efficient recognition pocket, and the latter tunes the recognition ability. Though not involved in the structural components of the cavity, the bulky mesityl groups hang over the cavity, reducing the effective volume and controlling the guest binding and motion. Since replacement of the ancillary ligands is straightforward, the unique functions of cages **1** can be rapidly elaborated using the present strategy.

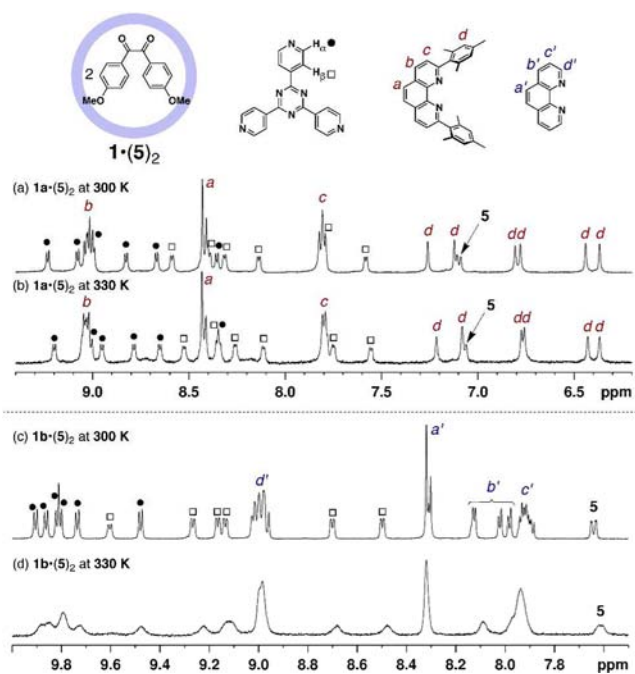


**Figure 5.** VT- $^1\text{H}$  NMR spectra (500 MHz,  $\text{D}_2\text{O}$ ) of (a,b) inclusion complex  $1\text{a}\cdot(5)_2$  and (c,d) inclusion complex  $1\text{b}\cdot(5)_2$ .

## ■ ASSOCIATED CONTENT

### Supporting Information

Experimental procedures, physical properties, and crystallographic data (CIF). This material is available free of charge via the Internet at <http://pubs.acs.org>.

## ■ AUTHOR INFORMATION

### Corresponding Author

[mfujita@appchem.t.u-tokyo.ac.jp](mailto:mfujita@appchem.t.u-tokyo.ac.jp)

### Notes

The authors declare no competing financial interest.

## ■ ACKNOWLEDGMENTS

This research was supported by a Grant-in-Aid for Specially promoted Research (24000009) and for Young Scientists (B) (23750057). The experiments of synchrotron X-ray crystallography were performed at the BL41XU and BL38B1 beamlines in the SPring-8 with the approval of the Japan Synchrotron Radiation Research Institute (JASRI) (Proposal Nos. 2012A0042 and 2012A0039).

## ■ REFERENCES

- (1) Hedstrom, L. *Chem. Rev.* **2002**, *102*, 4501.
- (2) Perona, J. J.; Craik, C. S. *Protein Sci.* **1995**, *4*, 337.
- (3) (a) Hedstrom, L.; Szilagyi, L.; Rutter, W. J. *Science* **1992**, *255*, 1249. (b) Hedstrom, L.; Perona, J. J.; Rutter, W. J. *Biochemistry* **1994**, *33*, 8757. (c) Hedstrom, L.; Farr-Jones, S.; Kettner, C. A.; Rutter, W. J. *Biochemistry* **1994**, *33*, 8764.
- (4) Remote chiral ancillary groups can affect the behaviors of achiral guests in the cavity of a synthetic host. See: (a) Castellano, R. K.; Kim, B. H.; Rebek, J., Jr. *J. Am. Chem. Soc.* **1997**, *119*, 12671. (b) Castellano, R. K.; Nuckolls, C.; Rebek, J., Jr. *J. Am. Chem. Soc.* **1999**, *121*, 11156. (c) Amaya, T.; Rebek, J., Jr. *J. Am. Chem. Soc.* **2004**, *126*, 6216. (d) Nishioka, Y.; Yamaguchi, T.; Kawano, M.; Fujita, M. *J. Am. Chem. Soc.* **2008**, *130*, 8160. (e) Murase, T.; Peschard, S.; Horiuchi, S.; Nishioka, Y.; Fujita, M. *Supramol. Chem.* **2011**, *23*, 199.

(5) Yoshizawa, M.; Klosterman, J. K.; Fujita, M. *Angew. Chem., Int. Ed.* **2009**, *48*, 3418.

(6) (a) Schmittl, M.; Lüning, U.; Meder, M.; Ganz, A.; Michel, C.; Herderich, M. *Heterocycl. Commun.* **1997**, *3*, 493. (b) Kalsani, V.; Ammon, H.; Jäckel, F.; Rabe, J. P.; Schmittl, M. *Chem.—Eur. J.* **2004**, *10*, 5481. (c) Schmittl, M.; He, B.; Fan, J.; Bats, J. W.; Engeser, M.; Schlosser, M.; Deiseroth, H. *Inorg. Chem.* **2009**, *48*, 8192.

(7) Burger, P.; Baumeister, J. M. *J. Organomet. Chem.* **1999**, *575*, 214.

(8) Kleywegt, G. J.; Jones, T. A. *Acta Crystallogr.* **1994**, *D50*, 178.

(9) For calculations of the cavity volumes of artificial self-assembled cages and capsules using the VOIDOO program, see: (a) Bilbeisi, R. A.; Clegg, J. K.; Elgrishi, N.; Hatten, X. D.; Devillard, M.; Breiner, B.; Mal, P.; Nitschke, J. R. *J. Am. Chem. Soc.* **2012**, *134*, 5110. (b) Riddell, I. A.; Smulders, M. M. J.; Clegg, J. K.; Hristova, Y. R.; Breiner, B.; Thoburn, J. D.; Nitschke, J. R. *Nat. Chem.* **2012**, *4*, 751. (c) Hristova, Y. R.; Smulders, M. M. J.; Clegg, J. K.; Breiner, B.; Nitschke, J. R. *Chem. Sci.* **2011**, *2*, 638. (d) Mugridge, J. S.; Bergman, R. G.; Raymond, K. N. *J. Am. Chem. Soc.* **2010**, *132*, 16256. (e) Mugridge, J. S.; Bergman, R. G.; Raymond, K. N. *J. Am. Chem. Soc.* **2011**, *133*, 11205. (f) Pluth, M. D.; Bergman, R. G.; Raymond, K. N. *J. Am. Chem. Soc.* **2007**, *129*, 94720. (g) Clegg, J. K.; Li, F.; Jolliffe, K. A.; Meehan, G. V.; Lindoy, L. F. *Chem. Commun.* **2011**, *47*, 6042.

(10) For the details of the cavity volume calculation of cages **1**, see the Supporting Information. Although the cavity volume of cage **1b** could not be calculated due to the poor crystal data, the volume is expected to be almost the same as that of cage **1c**.

(11) The estimated central void volumes are much smaller than the actual open cavity volumes containing the portal regions.

(12) Kusakawa, T.; Fujita, M. *Angew. Chem., Int. Ed.* **1998**, *37*, 3142.

(13) (a) Kusakawa, T.; Yoshizawa, M.; Fujita, M. *Angew. Chem., Int. Ed.* **2001**, *40*, 1879. (b) Kusakawa, T.; Fujita, M. *J. Am. Chem. Soc.* **2002**, *124*, 13576.